RAPID MANUFACTURING OF OSTE POLYMER RF-MEMS COMPONENTS

Sofia Rahiminejad[1], Jonas Hansson[2,3], Elof Köhler[1], Wouter van der Wijngaart[2], Tommy Haraldsson[2,3], Sjoerd Haasl[1,2] and Peter Enoksson[1]
[1]Chalmers University of Technology, Gothenburg, SWEDEN
[2]KTH Royal Institute of Technology, Stockholm, SWEDEN
[3]Mercene Labs AB, Stockholm, SWEDEN

ABSTRACT

This paper reports the first RF-MEMS component in OSTE polymer. Three OSTE-based ridge gap resonators were fabricated by direct, high aspect ratio, photostructuring. The OSTE polymer's good adhesion to gold makes it suitable for RF-MEMS applications. The OSTE ridge gap resonators differ in how they were coated with gold. The OSTE-based devices are compared to each other as well as to Si-based, SU8-based, and CNT-based devices of equal design. The OSTE-based process was performed outside the cleanroom, and with a fast fabrication process (~1 h). The OSTE-based device performance is on par with that of the other alternatives in terms of frequency, attenuation, and Q-factor.

INTRODUCTION

The rapid development of wireless technology increases the need for high-frequency components. Higher frequencies offer wider bandwidths and are needed for technologies such as high data rate wireless media communication [1], and automotive car radars [2].

At lower frequencies, electromagnetic components are typically made with micro-milling, which is an expensive serial manufacturing process. However, when designing these components at higher frequencies, above 100 GHz, micro-milling is lacking in resolution. Microfabrication of RF-MEMS components with structure sizes larger than 100 µm are typically manufactured with relatively slow and expensive processes, such as silicon etching, or SU8 lithography [3], and the processes have long design cycle iteration times, Tab. 1. There is a need for a fabrication method that can offer high aspect ratios, short design cycles, and low-cost processing.

Table 1. Comparison of manufacturing methods of RF components.

	Manufacturing methods			
	Si	**SU8**	**Milling**	**OSTE**
Low Cost	-	+	- -	+ +
Time	+	+	-	+ +
Mass producible	+	+	- -	+
Au adhesion	+	-	-	+ +

In 2011 a new polymer the Off-Stoichiometry Thiol-Ene (OSTE) polymer was designed for fabrication of microfluidic devices [4]. The OSTE polymer's reactive surface allows easy manufacturing of multilayer devices with low stress and low deformation [5]. The material allows fast prototyping by high aspect ratio direct photostructuring [6]. OSTE components can be reaction injection molded with short cycle times [5], allowing for scaling up of component production. Compared to the polymer SU8, the OSTE polymer's mechanical properties can be tuned to be stiff or flexible [4], and contains sulfur, which enables easy bonding of gold to OSTE.

In this paper the first RF-MEMS component in OSTE polymer has been fabricated and evaluated. The OSTE polymer is used to fabricate a ridge gap resonator operating at 280 GHz [7]. The OSTE-based resonator is compared to previous Si-based [7], SU8-based [8] and carbon nanotubes (CNT) -based [9] ridge gap resonators of equal design.

DESIGN

The ridge gap resonator is based on gap waveguide technology. By using a metamaterial that forms an artificial magnetically conductive (AMC) surface, together with a perfect electrically conductive (PEC) surface less than a quarter wavelength apart, a stop band for a certain frequency range can be achieved [10]. Here, the AMC surface is a "bed of nails" [11]. By incorporating a guiding structure in between the AMC, in this case a ridge, the waves can propagate along the ridge without leaking away.

The resonator consists of a conductive ridge surrounded by an AMC surface. On the long sides of the ridge, two rows of pins are present to create the stopband, and on the short sides of the ridge (the connecting sides), only one row of pins is present. The conductive lid is placed 167 µm above the ridge. The pins and the ridge are 329 µm high. The ridge is 2059 µm long and the pins are 167 µm wide.

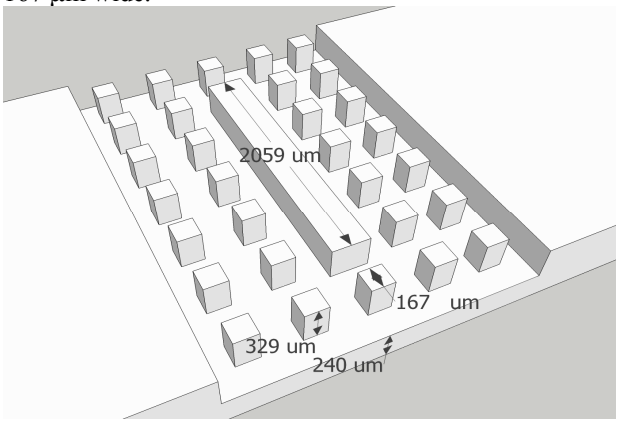

Figure 1: Schematic illustration of the gap waveguide resonator, displaying the dimensions and placements of the pin and the ridge.

FABRICATION

The 280 GHz ridge gap resonator is fabricated in two layers of OSTE polymer followed by a gold coating. The fabrication process is presented in Fig. 2.

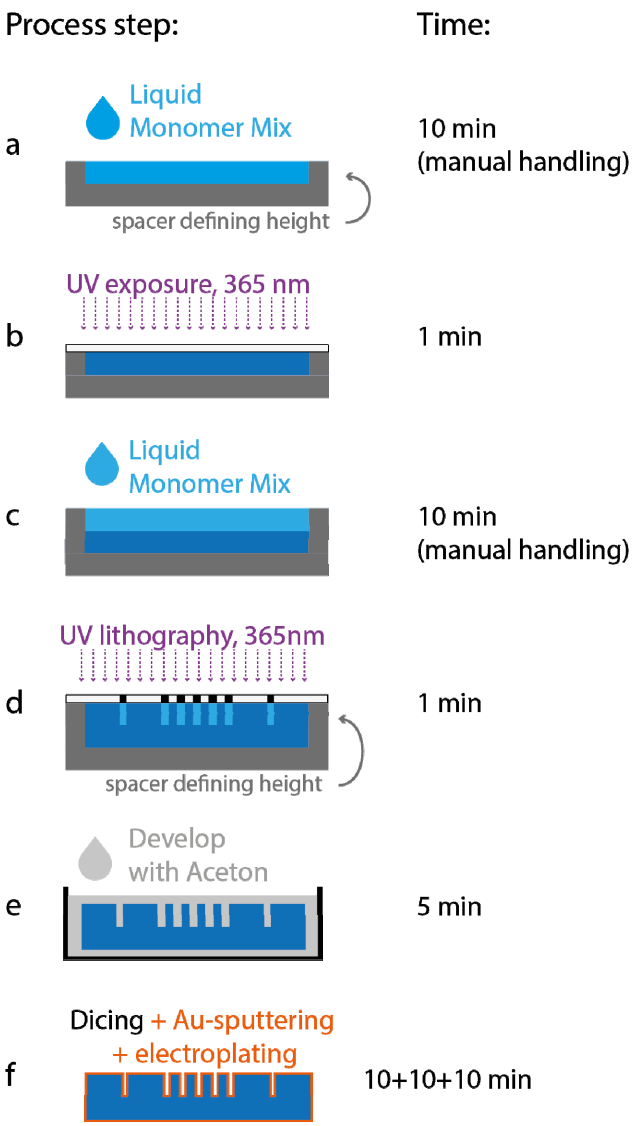

Figure 2: ***Manufacturing process****, showing the process steps and respective process time.*

The entire device is formed using two different OSTE polymers. An unstructured base layer is made in *Ostemer 221*, that provides good bonding properties to the microstructured layer and a relatively high Young's modulus. The microstructured layer uses *Ostemer 220 Litho*, in order to obtain good lithographic definition.

For the base layer, 240 µm spacers are placed on a microscope glass slide and *Ostemer 221* (Mercene Labs AB, Sweden) is poured onto the microscope glass, Fig 2a. The polymer is squeezed by a top lid consisting of another microscope glass and a transparency film in between. The layer is UV cured (Collimated Hg-lamp, OAI, Millpitas, USA) for 60 sec at 10 mW/cm^2 at 365 nm. Fig. 2b. The top transparency film and microscope glass is removed, leaving a flat UV cured *Ostemer 221* surface. 390 µm thick spacers are placed on the *Ostemer 221*, and the polymer *Ostemer 220 Litho* (Mercene Labs, Sweden) is poured on top, Fig. 2c. Both layers are now squeezed by a photomask consisting of a microscope glass with a repro-printed transparency film. The photomask is protected by a Teflon film to avoid stiction of the polymer to the mask. The entire stack is placed on top of black paper during UV exposure (365 nm) to avoid reflection. The stack is UV exposed for 60 sec, Fig. 2d. The photomask is removed and the polymer stack is developed in an acetone bath with ultrasonic agitation for 3 min, Fig. 2e. The OSTE stack is sputtered with a seed layer of 180 nm Au from the top. Unlike all polymer alternatives, OSTE contains sulfur that enables direct covalent bonding to gold, resulting in very strongly attached gold layers, therefore no adhesion layer such as Ti or Cr is needed. The OSTE stack, including the microscope glass, is electroplated in a gold ion solution (Enthrone Neutronex) for 5 min at 38 °C, still attached to the microscope glass. The bottom microscope glass is removed and the OSTE-based resonators are diced with a diamond saw into separate chips. Three OSTE chips (A, B, and C) was processed with slightly different coating parameters. Each chip is sputtered with a seed layer of 180 nm Au from the back. OSTE chip A and OSTE chip B were electroplated for 5 min, at 43 °C and 40 °C respectively. OSTE chip C was not electroplated a second time, Fig. 2f.

Figure 3: Photo of the Au coated OSTE polymer device.

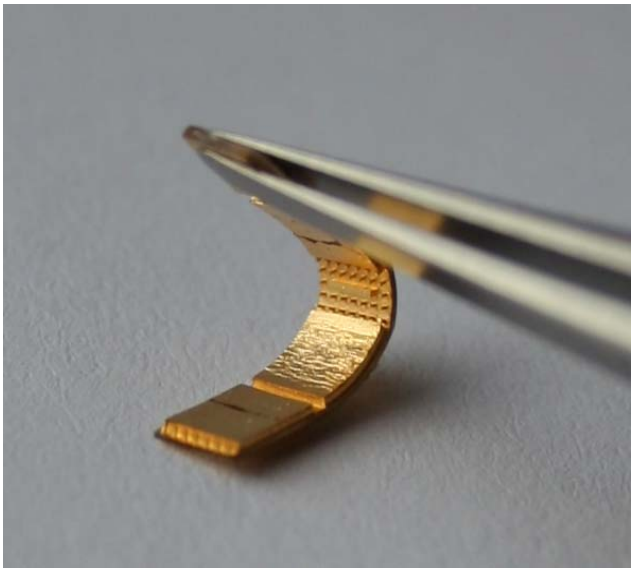

Figure 4: Demonstration of flexibility and gold plating quality.

The entire device fabrication was performed in around 1 hour. In comparison, just the pure processing

time for the SU8 device in [8] (curing, exposure and agitation) was more than 4 h in total. The fabricated OSTE-based gold-covered ridge gap resonator is presented in Fig. 3.

The device was bent several times without any visible signs of cracks or the Au peeling off. The OSTE polymer can also be tuned to be stiff if desired. The flexibility of the OSTE-based ridge gap resonator is displayed in Fig. 4.

MEASUREMENT RESULTS

The OSTE-based resonators were compared to previous resonators of the same design in Si, SU8 and CNT, the attenuation was extracted from the resonances as in [12].

The three OSTE-based ridge gap resonators were measured between 220-325 GHz. Two resonance peaks were detected for all three devices, the measurements together with the simulated data of an ideal ridge gap resonator, is presented in Fig. 5 and Fig. 6.

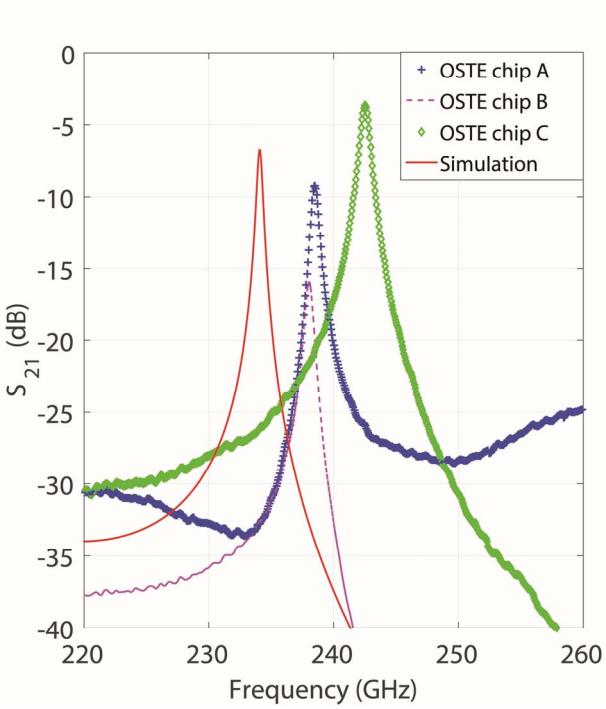

*Figure 5: **Measurements results** of the three OSTE resonators and the simulations at 220-260 GHz*

The loaded Q-values (Q_L) were extracted from the measured resonances. Q_L is defined as the ratio between the center frequency of the resonant cavity and its 3-dB bandwidth, Eq. 1, [13].

$$Q_L = \frac{f_c}{\Delta f_{3dB}} \quad (1)$$

The unloaded Q (Q_U) is calculated by Eq. 2,

$$Q_U = \frac{Q_L}{1-10^{-S21(dB)/20}} \quad (2)$$

and the attenuation α is calculated by Eq. 3.

$$\alpha = \frac{\beta}{2Q_U} \quad (3)$$

Where the β is the propagation constant. The calculated Q_U-values and attenuation values for the OSTE-based resonators, together with measured values for the previous Si-based, SU8-based and CNT-based resonators, are presented in Tab. 2.

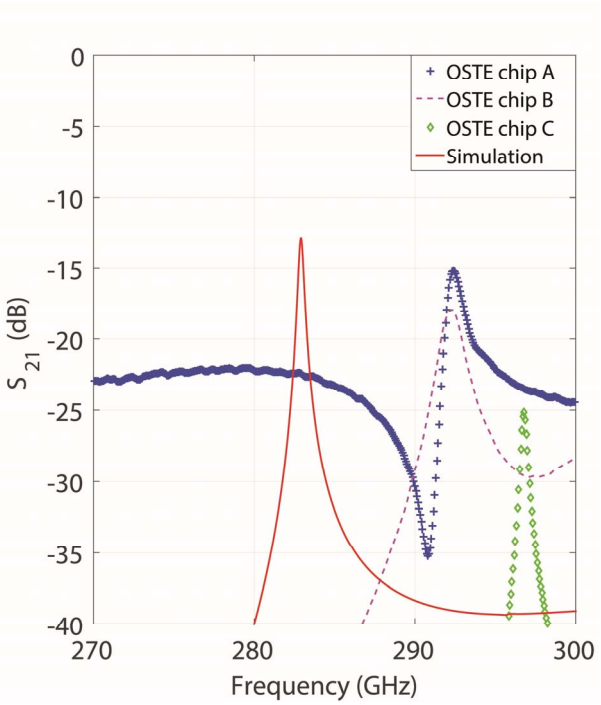

*Figure 6: **Measurements results** of the three OSTE resonators and the simulations at 270-300 GHz.*

DISCUSSION

The three chips, OSTE A, OSTE B and OSTE C, showed different attenuation. This is probably due to different quality of the Au surface. OSTE chip C, which showed the lowest attenuation, was only electroplated once, and had a surface roughness of 320 nm. OSTE chip A, which was electroplated twice, showed a surface roughness of 680 nm. OSTE chip C's attenuation shows the best performance compared to the previously reported Si, SU8 and CNT ridge gap resonators. However, the OSTE ridge gap resonators are all within the same order of magnitude as the simulated values and the previously reported values.

CONCLUSION

The first RF-MEMS component in OSTE polymer has been presented. The attenuation of the OSTE resonators differ somewhat from each other, due to differences in the gold-coating process step, but they are as good as previously reported resonators in other materials. The OSTE resonators with the lowest measured attenuation performed better than previous reported resonators at values comparable to simulations of an ideal ridge gap resonator. The OSTE process is fast compared to other know processes. Additionally, no cleanroom is

*Table 2. **Performance comparison** of the unloaded Q-values and losses from the OSTE resonators (chip A, B, C), simulations, and previous devices in Si, SU8 and CNT of identical design.*

	Materials						
	Simulation	**Si[8]**	**SU8[8]**	**CNT [9]**	**OSTE A**	**OSTE B**	**OSTE C**
Frequency (GHz)	234	234	233	236	239	238	243
Q_u-value	859	642	319	274	608	314	782
Loss (dB/mm)	0.025	0.033	0.067	0.079	**0.036**	**0.064**	**0.028**
Frequency (GHz)	284	284	283	289	292	292	297
Q_u-value	992	597	628	518	308	210	785
Attenuation (dB/mm)	0.026	0.043	0.041	0.051	**0.087**	**0.127**	**0.034**

needed to perform the process, the process is mass producible, and OSTE's good adhesion to gold offers many applications for RF MEMS.

ACKNOWLEDGEMENTS

The authors would like to acknowledge the Swedish Research Council VR Grant Number C0466101, and the Chalmers production area of advanced science for funding of the reported work.

REFERENCES

[1] N. Kukutsu, A. Hirata, M. Yaita, K. Ajito, H. Takahashi, T. Kosugi, H.-J. Song, A. Wakatsuki, Y. Muramoto, T. Nagatsuma, and Y. Kado, "Toward practical applications over 100 GHz," IEEE MTT-S International in Microwave Symposium Digest (MTT), 2010, Anaheim, 2010, pp. 1134–1137.

[2] J. Hasch, E. Topak, R. Schnabel, T. Zwick, R. Weigel, and C. Waldschmidt, "Millimeter-wave technology for automotive radar sensors in the 77 GHz frequency band," IEEE Transactions on Microwave Theory and Techniques, vol. 60, no. 3 PART 2, pp. 845–860, 2012.

[3] X. Shang, M. Ke, Y. Wang, and M. J. Lancaster, "WR-3 Band Waveguides and Filters Fabricated Using SU8 Photoresist Micromachining Technology," IEEE Transactions on Terahertz Science and Technology, vol. 2, no. 6, pp. 629–637, 2012.

[4] C. F. Carlborg, T. Haraldsson, K. Öberg, M. Malkoch, and W. van der Wijngaart, "Beyond PDMS: off-stoichiometry thiol–ene (OSTE) based soft lithography for rapid prototyping of microfluidic devices," *Lab Chip*, vol. 11, no. 18, p. 3136, 2011.

[5] N. Sandström, R. Z. Shafagh, C. F. Carlborg, T. Haraldsson, G. Stemme, and W. Van Der Wijngaart, "One Step Integration Of Gold Coated Sensors With OSTE Polymer Cartridges By Low Temperature Dry Bonding," J. Micromechanics Microengineering, vol. 25, no. 7, p. 75002, 2015.

[6] M. Hillmering, G. Pardon, A. Vastesson, O. Supekar, C. F. Carlborg, B. D. Brandner, W. van der Wijngaart, and T. Haraldsson, "Off-stoichiometry improves the photostructuring of thiol–enes through diffusion-induced monomer depletion," *Microsystems Nanoeng.*, vol. 2, p. 15043, Feb. 2016.

[7] S. Rahiminejad, A. U. A. U. Zaman, E. Pucci, H. Raza, V. Vassilev, S. Haasl, P. Lundgren, P.-S. P.-S. Kildal, and P. Enoksson, "Micromachined ridge gap waveguide and resonator for millimeter-wave applications," *Sensors Actuators A Phys.*, vol. 186, pp. 264–269, Oct. 2012.

[8] S. Rahiminejad, E. Pucci, S. Haasl, and P. Enoksson, "SU8 ridge-gap waveguide resonator," *Int. J. Microw. Wirel. Technol.*, vol. 6, no. 5, pp. 459–465, May 2014.

[9] A. M. M. Saleem, S. Rahiminejad, V. Desmaris, and P. Enoksson, "Carbon nanotubes as base material for fabrication of gap waveguide components," *Sensors Actuators, A Phys.*, vol. 224, pp. 163–168, 2015.

[10] E. Rajo-Iglesias and P. S. Kildal, "Numerical studies of bandwidth of parallel-plate cut-off realised by a bed of nails, corrugations and mushroom-type electromagnetic bandgap for use in gap waveguides," in IET Microwaves, Antennas & Propagation, vol. 5, no. 3, pp. 282-289, Feb. 21 2011.

[11] M. G. Silveirinha, C. A. Fernandes and J. R. Costa, "Electromagnetic Characterization of Textured Surfaces Formed by Metallic Pins," in IEEE Transactions on Antennas and Propagation, vol. 56, no. 2, pp. 405-415, Feb. 2008.

[12] E. Pucci, A. U. Zaman, E. Rajo-Iglesias, P. S. Kildal and A. Kishk, "Study of Q-factors of ridge and groove gap waveguide resonators," in IET Microwaves, Antennas & Propagation, vol. 7, no. 11, pp. 900-908, August 20 2013.

[13] D. M Pozar, "Microwave Engineering, 3rd," JOHN WILEY SONS INC, 2005.

CONTACT

*P.E: Public, tel: +46 (0)31 772 1868;
peter.enoksson@chalmers.se